Cross-evaluation of GEMS tropospheric ozone retrieval performance using OMI data and the use of ozonesonde dataset over East Asia for validation

Juseon Bak[1,#] (Juseon.bak@cfa.harvard.edu)

Kang-Hyeon Baek[1] (iambk100@gmail.com) **Jae-Hwan Kim**[1, *] (jakim@pusan.ac.kr)

Xiong Liu[2] (xliu@cfa.harvard.edu), **Jhoon Kim**[3] (jkim2@yonsei.ac.kr) **Kelly Chance**[2]

(kchance@cfa.harvard.edu)

[1] Atmospheric Science Department, Pusan National University, Busan, Korea

[2] Atomic and Molecular Physics Division, Harvard-Smithsonian Center for Astrophysics, Cambridge, MA, USA

[3] Department of Atmospheric Sciences, Yonsei University, Seoul, Korea

[#]Currently at Atomic and Molecular Physics Division, Harvard-Smithsonian Center for Astrophysics, Cambridge, MA, USA

[*]Corresponding Author

16   **Abstract**

18   The Geostatioary Environment Monitoring Spectrometer (GEMS) is scheduled to be launched in 2019

19   on board the GEO-KOMPSAT (GEOstationary KOrea Multi-Purpose SATellite)-2B, contributing as

20   the Asian partner of the global geostationary constellation of air quality monitoring. To support this air

21   quality satellite mission, we perform a cross-evaluation of simulated GEMS ozone profile retrievals

22   from OMI (Ozone Monitoring Instrument) data based on the Optimal Estimation and ozonesonde

23   measurements within the GEMS domain, covering from 5°S (Indonesia) to 45°N (south of the Russian

24   border) and from 75°E to 145°E. The comparison between ozonesonde and GEMS shows a significant

25   dependence on ozonesonde types. Ozonesonde data measured by Modified Brewer-Master (MBM) at

26   Trivandrum and New Delhi show inconsistent seasonal variabilities in tropospheric ozone compared to

27   Carbon Iodine (CI) and Electrochemical Condensation Cell (ECC) ozonesondes at other stations in a

28   similar latitude regime. CI ozonesonde measurements are negatively biased relative to ECC

29   measurements by 2-4 DU; better agreement is achieved when simulated GEMS ozone retrievals are

30   compared to ECC measurements. ECC ozone data at Hanoi, Kuala Lumpur, and Singapore show

31   abnormally worse agreements with simulated GEMS retrievals than other ECC measurements.

32   Therefore, ECC ozonesonde measurements at Hong Kong, Pohang, Naha, Sapporo, and Tsukuba are

33   finally identified as an optimal reference dataset. The accuracy of simulated GEMS retrievals is

34   estimated to be ~ 5.0 % for both tropospheric and stratospheric column ozone with the precision of 15 %

35   and 5 %, which meets the GEMS ozone requirements.

36

1. Introduction

The development of geostationary ultraviolet (UV)/visible (VIS) spectrometers is a new paradigm in the field of the space-based air quality monitoring. It builds on the polar-orbiting instrument heritage for the last 40 years, which were initiated with the launch of a series of Total Ozone Mapping Spectrometer (TOMS) instruments starting in 1978 (Bhartia et al., 1996) and consolidated by the Global Ozone Monitoring Experiment (GOME) (ESA, 1995), the SCanning Imaging Absorption spectroMeter for Atmospheric CHartographY (SCIAMACHY) (Bovensmann et al., 1999), the Ozone Monitoring Instrument (OMI) (Levelt et al, 2006), GOME-2 (EUMETSAT, 2006), the Ozone Mapping and Profiler Suite (OMPS) (Flynn et al., 2014), and the TROPOspheric Monitoring Instrument (TROPOMI) (Veefkind et al., 2012). Three geostationary air quality monitoring missions, including the Geostationary Environmental Monitoring Spectrometer (GEMS) (Bak et al., 2013a) over East Asia, Tropospheric Emissions: Monitoring of Pollution (TEMPO) (Chance et al, 2013; Zoogman et al., 2017) over North America, and Sentinel-4 (Ingmann et al., 2012) over Europe, are in progress to launch in the 2019-2022 time frame, to provide unprecedented hourly measurements of aerosols and chemical pollutants at sub-urban scale spatial resolution (~ 10-50 km^2). These missions will constitute the global geostationary constellation of air quality monitoring.

GEMS will be launched in late 2019 or early 2020 on board the GeoKOMPSAT-2B (Geostationary Korea Multi-Purpose Satellite) to measure O_3, NO_2, SO_2, H_2CO, CHOCHO, and aerosols in East Asia (Bak et al., 2013a). Tropospheric ozone is a key species to be monitored due to its critical role in controlling air-quality as a primary component of photochemical smog, its self-cleansing capacity as a precursor of the hydroxyl radical, and in controlling the Earth's radiative balance as a greenhouse gas.

To support the development of the GEMS ozone profile algorithm, Bak et al. (2013a) demonstrated that the GEMS spectral coverage of 300-500 nm minimizes the loss in the sensitivity to tropospheric ozone despite the lack of most Hartley ozone absorption wavelengths shorter than 300 nm. They further indicated the acceptable quality of the simulated stratospheric ozone retrievals from 212 hPa to 3 hPa (40 km) through comparisons using Microwave Limb Sounder (MLS) measurements. As a consecutive work, this study evaluates simulated GEMS tropospheric ozone retrievals against ozonesonde observations. GEMS ozone retrievals are simulated using an Optimal Estimation (OE) based fitting algorithm with OMI radiances in the spectral range 300-330 nm in the same way as Bak et al. (2013a). The validation effort is essential to ensuring the quality of GEMS ozone profile retrievals and to verifying the newly implemented ozone profile retrieval scheme. In-situ ozonesonde soundings have been considered to be the best reference, but should be carefully used due to the spatial and temporal

irregularities in instrument types, manufacturers, operating procedures, and correction strategies (Deshler et al., 2017). Compared to TEMPO and Sentinel-4, the GEMS validation activity is expected to be more challenging for the ozone profile product because of the much sparser distribution of stations and more irregular characteristics of ozonesonde measurements over the GEMS domain. Continuous balloon-borne observations of ozone are only available at the Pohang (129.23°E, 36.02°N) site in South Korea, but this site has not been thoroughly validated. Therefore the quality assessment of its ozonesonde data is required before we use this data for GEMS validation. Compared to ozonesondes, satellite ozone data are less accurate and have much coarser vertical resolution, but more homogenous due to single data processing for the measurements from a single instrument. Therefore, abnormal deviations in satellite-ozonesonde differences from neighboring stations might indicate problems at individual stations (Fioletov et al. 2008). For example, Bak et al. (2015) identified 27 homogenous stations among 35 global Brewer stations available from the World Ozone and Ultraviolet Radiation Data Centre (WOUDC) network through comparisons with coincident OMI total ozone data. This study adopts this approach to select a consistent ozonesonde dataset among 10 stations available over the GEMS domain based on comparisons of the tropospheric ozone columns (TOC) between simulated GEMS retrievals and ozonesonde measurements, that is, simulated GEMS retrievals using OMI data are used to verify the ozonesonde observations. The simulated GEMS retrievals are ultimately evaluated against the ozonesonde dataset identified as a true reference to demonstrate the reliability of our future GEMS ozone product. The simulated GEMS retrievals and ozonesonde dataset are described in Sect. 2.1 and 2.2 with the comparison methodology in Sect. 2.3. Our results are discussed in Sect. 3 and summarized in Sect. 4.

2. Data and Methodology

2.1 Ozone Profile Retrievals

The development of the GEMS ozone profile algorithm builds on the heritage of the Smithsonian Astrophysical Observatory (SAO) ozone profile algorithm which was originally developed for GOME (Liu et al., 2005), continuously adapted for its successors including OMI (Liu et al., 2010a), GOME-2 (Cai et al., 2012), and OMPS (Bak et al., 2017). In addition, the SAO algorithm will be implemented to retrieve TEMPO ozone profiles (Chance et al., 2013; Zoogman et al., 2017). In this algorithm, the well-known optimal estimation (OE) based iterative inversion is applied to estimate the best ozone concentrations from simultaneously minimizing between measured and simulated backscattered UV

103 measurements constrained by the measurement covariance matrix, and between retrieved values and its

104 climatological a priori values constrained by an a priori covariance matrix (Rodgers, 2000). The impact

105 of a priori information on retrievals becomes important when measurement information is reduced due

106 to instrumental errors, instrument design sensitivity (e.g. stray light, dark current, and read-out smear),

107 and physically insufficient sensitivities under certain geophysical conditions (e.g. the reduced

108 penetration of incoming UV radiation into the lower troposphere at high solar zenith angles or blocked

109 photon penetration below thick clouds). The described OE-fitting solution $\hat{X}_{i+1}$ can be written,

110 together with cost function χ^2:

111

112
$$\hat{X}_{i+1} = \hat{X}_i + \left(K_i^T S_y^{-1} K_i + S_a^{-1}\right)^{-1} \{K_i^T S_y^{-1}[Y - R(\hat{X}_i)] - S_a^{-1}(\hat{X}_i - X_a)\} \qquad (1)$$

113

114
$$\chi^2 = \left\| S_y^{-\frac{1}{2}} K_i(\hat{X}_{i+1} - \hat{X}_i) - [Y - R(\hat{X}_i)] \right\|_2^2 + \left\| S_a^{-\frac{1}{2}}(\hat{X}_{i+1} - X_a) \right\|_2^2, \qquad (2)$$

115

116 where $\hat{X}_{i+1}$ and $\hat{X}_i$ are current and previous state vectors with a priori vector, X_a and its covariance

117 error matrix, S_a. Y and R(X) are measured and simulated radiance vectors, with measurement error

118 covariance matrix, S_y. K is the weighting function matrix ($\frac{dR(x)}{dx}$), describing the sensitivity of the

119 forward model to small perturbations of the state vector.

120 The ozone fitting window was determined to maximize the retrieval sensitivity to ozone and

121 minimize it to measurement error: 289–307 nm and 326–339 nm for GOME, 270-309 nm and 312-330

122 nm for OMI, 289−307 nm and 325−340 nm for GOME-2, and 302.5-340 nm for OMPS. For OMI,

123 GOME and GOME-2, partial ozone columns are typically retrieved in 24 layers from the surface to ~

124 60 km. However, GEMS (300-500 nm) and OMPS (300-380 nm) do not cover much of the Hartley

125 ozone absorption wavelengths and hence the reliable profile information of ozone is limited to below ~

126 40 km (Bak et al., 2013a).

127 Fig. 1 is a schematic diagram of the ozone profile algorithm. With the input of satellite

128 measurements, the slit function is parameterized through cross-correlation between satellite irradiance

129 and a high-resolution solar reference spectrum to be used for wavelength calibration and for high -

130 resolution cross section convolution (Sun et al., 2017; Bak et al., 2017); a normalized Gaussian

131 distribution is assumed to derive analytic slit functions for OMI. To remove the systematic errors

132 between measured and calculated radiances, "soft-calibration" is applied to measured radiances and

133 then the logarithms of sun-normalized radiances are calculated as measurement vectors (Liu et al.,

134   2010a; Cai et al., 2012; Bak et al., 2017). Measurement covariance matrices are constructed as diagonal

135   matrices with components taken from the square of the measurement errors as measurement errors are

136   assumed to be uncorrelated among wavelengths. In the OMI algorithm, a noise floor of 0.4 % (UV1)

137   and 0.2 % (UV2) is used because OMI measurement errors underestimate other kinds of random noise

138   errors caused by stray light, dark current, geophysical pseudo-random noise errors due to sub-pixel

139   variability, motion when taking a measurement, forward model parameter error (random part), and other

140   unknown errors into account (Huang et al., 2017). GEMS is expected to have similar retrieval sensitivity

141   to tropospheric ozone, and have at least comparable radiometric/wavelength accuracy (4% including

142   light source uncertainty/0.01 nm) as OMI. It is desgined to provide hyperspectral radiances at a spectral

143   resolution of 0.6 nm and spectral intervals of 0.2 nm, which are also similar to OMI (spectral resolution:

144   0.42-0.63 nm, sampling rate: 0.14-0.33 nm/pixel). A priori ozone information is taken from the

145   tropopause-based (TB) ozone profile climatology which was developed for improving ozone profile

146   retrievals in the upper troposphere and lower stratosphere (Bak et al., 2013b). The Vector LInearized

147   Discrete Ordinate Radiative Transfer (VLIDORT) model (Spurr, 2006; 2008) is used to calculate

148   normalized radiances and weighting function matrices for the atmosphere, with Rayleigh scattering and

149   trace-gas absorption and with Lambertian reflection for both surface and cloud (Liu et al., 2010a). The

150   ozone algorithm iteratively estimates the best ozone profiles within the retrieval converges (typically 2-

151   3 iterations), together with other geophysical and calibration parameters (e.g., cloud fraction, albedo,

152   BrO, wavelength shift, Ring parameter, mean fitting scaling parameter) for a better fitting accuracy

153   even though some of the additional fitting parameters can reduce the degrees of freedom for signal of

154   ozone. We should note here that GEMS data processing is expected to be different from OMI mainly

155   in two ways: 1) OMI uses a depolarizer to scramble the polarization of light. However, GEMS has

156   polarization sensitivity (required to be less than 2%) and performs polarization correction using an

157   RTM-based look-up table of atmospheric polarization state and pre-flight characterization of instrument

158   polarization sensitivity in the level 0 to 1b data processing. The GEMS polarization correction is less

159   accurate and hence additional fitting process might be required in the level 2 data processing, especially

160   for ozone profiles that are more sensitive to the polarization error compared to other trace-gases. 2)

161   GEMS has a capability to perform diurnal observations and hence diurnal meteorological input data are

162   required to account for the temperature dependent Huggins band ozone absorption. Hence, the

163   numerical weather prediction (NWP) model analysis data will be transferred to the GEMS Science Data

164   Processing Center (SDPC).

165

166   **2.2 Ozonesonde measurements**

167

168   Ozonesondes are small, lightweight, and compact balloon-borne instruments capable of measuring
169   profiles of ozone, pressure, temperature and humidity from the surface to balloon burst, usually near 35
170   km (4 hPa); ozone measurements are typically reported in units of partial pressure (mPa) with vertical
171   resolution of ~ 100-150 m (WMO, 2014). Ozone soundings have been taken for more than 50 years,
172   since the 1960s. The accuracy of ozonesonde measurements has been reported as 5-10 % with precision
173   of 3-5%, depending on the sensor type, manufacturer, solution concentrations, and operational
174   procedure (Smit et al., 2007; Thompson et al., 2007; 2017; Witte et al., 2017; 2018). Three types of
175   instruments have been carried on balloons, i.e., the modified Brewer-Master (MBM), the carbon iodine
176   cell (CI), and the electrochemical concentration cell (ECC). Each sounding is disposably operated and
177   hence weekly launched for long-term operation.

178   Fig. 2 displays the locations of 10 ozonesonde sites focused on this study within the GEMS domain
179   bordering from 5°S (Indonesia) to 45°N (south of the Russian border) and from 75°E to 145°E. A
180   summary of each ozonesonde site is presented in Table 1. Most of measurements are collected from the
181   WOUDC network, except that Pohang soundings are provided from the Korea Meteorological
182   Administration (KMA) and Kuala Lumpur and Hanoi measurements are from the Southern Hemisphere
183   Additional OZonesondes (SHADOZ) network. In South Korea, ECC sondes have been launched every
184   Wednesday since 1995 at Pohang, without significant time gaps. There are three Japanese stations (Naha,
185   Tsukuba, and Sapporo) where the CI-type sensor was used before switching to the ECC-type sensor as
186   of early 2009, and two Indian stations at New Delhi and Trivandrum using the modified BM (MBM)
187   sensor. The rest of stations (Hanoi, Hong Kong, Kuala Lumpur and Singapore) use only ECC. Most
188   stations employ ECC sensors, but inhomogeneities in ECC ozonesondes are strongly correlated to
189   preparation and correction procedures. There are two ECC sensor manufactures: the Science Pump
190   Corporation (Model type: SPC-6A) and the Environmental Science Corporation (Model type: EN-SCI-
191   Z/1Z/2Z). Since 2011 EN-SCI has been taken over by Droplet Measurement Technologies (DMT) Inc.
192   The the recommend recipes of the Standard Sensing Solution (SSI) are 1.0 % potassium iodide (KI)/full
193   buffer (SST1.0) and 2.0 % KI/no buffer (SST0.5) for the SPC and EN-SCI sondes, respectively by the
194   ASOPOS (Assessment for Standards on Operation Procedures for Ozone Sondes) (Smit et al., 2012).
195   Among ECC stations, Pohang, Hong Kong, and the Japanese stations have applied the standard sensing
196   solution to all ECC sensors manufactured by one company. In Singapore, the ozonesonde manufacture
197   was changed in late 2015 from EN-SCI to SPC, while SST 0.5 was switched to SST1.0 as of 2018. Two
198   SHADOZ stations (Kuala Lumpur, Hanoi) have applied the standard sensing solution just since 2015.
199   Hanoi changed sensing solution 4 times with two different ozonesonde manufactures; Kuala Lumpur

200 operated only with SPC 6A-SST1.0 combination until 2014, but with four different radiosonde
201 manufactures. Therefore the SHADOZ datasets were homogenized (Witte et al., 2017) through the
202 application of transfer functions between sensors and solution types. The post-processing could be
203 applied by data users to some WOUDC datasets given a correction factor, which is the ratio of integrated
204 ozonesonde column (appended with an estimated residual ozone column above burst altitude) and total
205 ozone measurements from co-located ground-based and/or overpassing satellite instruments. The
206 above-burst column ozone is estimated with a constant ozone mixing ratio (CMR) assumption above
207 the burst altitude (Japanese sites, Morris et al., 2013) or satellite derived stratospheric ozone climatology
208 (Indian sites, Rohtash et al., 2016). No post-processing is done for Pohang, Hong Kong, and Singapore.
209 Most stations made weekly or bi-weekly regular observations, except for Indian stations with irregular
210 periods of 0-4 per month and for Singapore with monthly observations.

211   In Fig. 3 the seasonal means and standard deviations of ozonesonde measurements are
212 presented to show the stability and characteristics of ozonesonde measurements at each site.
213 Instabilities of measurements are observed from New Delhi ozonesondes. High surface ozone
214 concentrations at Trivandrum in summer are believed to be caused by measurement errors
215 because low levels of pollutants have been reported at this site under these geolocation and
216 meteorological effects (Lal et al. 2000). Besides Trivandrum, Naha could be regarded as a
217 background site according to low surface ozone (Fig. 3) and precursor concentrations (Fig. 2)
218 compared to neighboring stations, and previous studies (Oltmans et al., 2004; Liu et al., 2002).
219 In the lower troposphere, high ozone concentrations are captured at Pohang, Tsukuba, and
220 Sapporo in the summer due to enhanced photochemical production of ozone in daytime,
221 whereas tropical sites, Naha, Hanoi, and Hong Kong show ozone enhancements in spring,
222 mainly due to biomass burning in Southeast Asia, with low ozone concentrations in summer
223 due to the Asian monsoon and in winter due to tropical air intrusion (Liu et al., 2002; Ogino et
224 al., 2013). Singapore and Kuala Lumpur are supposed to be severely polluted areas, but ozone
225 pollution is not clearly captured over the seasons. This might be explained by the morning
226 observation time at these two stations. In addition, instabilities of Singapore measurements are
227 noticeable, including abnormally large variability and very low ozone concentration in the
228 stratosphere. The effect of stratospheric intrusions on the ozone profile shape is dominant at
229 mid-latitudes (Pohang, Tsukuba, and Sapporo) during the spring and winter when the
230 ozonepause goes down to 300 hPa, with larger ozone variabilities in the lower stratosphere and
231 upper troposphere, whereas the ozonepause is around 100 hPa with much less variability of

232   ozone in other seasons.

233

234   **2.3. Comparison Methodology**

235

236   The GEMS ozone profile algorithm is applied to OMI BUV measurements for 300-330 nm to

237   simulate GEMS ozone profile retrievals at coincident locations listed in Table 1. The coincidence

238   criteria between satellite and ozonesondes are: $\pm1.0^{\circ}$ in both longitude and latitude and ±12 hours in

239   time, and then the closest pixel is selected. The Aura satellite carrying OMI crosses the equator always

240   at ~ 1:45 pm Local Time (LT), thus OMI measurements are collocated within 3 hours to ozonesonde

241   soundings in the afternoon (1-3 pm). Weekly-based sonde measurements provide 48 ozone profiles at

242   maximum for a year; the number of collocations is on average 40 from 2004 October to 2008, but

243   reduced to ~ 20 recently due to the screened OMI measurements affected by the "row anomaly" which

244   was initially detected at two rows in 2007, and seriously spread to other rows with time since January

245   2009 (Schenkeveld et al., 2017). From July 2011 the row anomaly extends up to ~ 50 % of all rows.

246   Correspondingly, the average collocation distance increases from 57.5 km to 66.6 km before and after

247   the occurrence of the row anomaly. The impact of spatiotemporal variability on the comparison will be

248   much reduced for GEMS due to its higher spatiotemporal resolution (7 km × 8 km @ Seoul, hourly)

249   against OMI (48 km × 13 km @ nadir in UV1, daily).

250   To increase the validation accuracy, data screening is implemented for both ozonesonde

251   observations and satellite retrievals according to Huang et al (2017). For ozonesonde observations, we

252   screen ozonesondes with balloon-bursting pressures exceeding 200 hPa, gaps greater than 3 km,

253   abnormally high concentration in the troposphere (> 80 DU), and low concentration in the stratosphere

254   (<100 DU). Among WOUDC sites, the Japanese and Indian datasets include a correction factor which

255   is derived to make better agreement between integrated ozonesonde columns and correlated reference

256   total ozone measurements as mentioned in Section 2.2; In Fig. 4, Japanese ozonesondes are compared

257   against GEMS simulations when a correction factor is applied or not to each CI and ECC measurement,

258   respectively. Morris et al. (2013) recommended restricting the application of this correction factor to

259   the stratospheric portion of the CI ozonesonde profiles due to errors in the above-burst column ozone.

260   Our comparison results illustrate that applying the correction factor reduces the vertical fluctuation of

261   mean biases in ozone profile differences with insignificant impact on their standard deviations.

262   Therefore we decide to apply this correction factor to the sonde profiles if this factor ranges from 0.85

263   to 1.15. Because of a lack of retrieval sensitivity to ozone below clouds and lower tropospheric ozone

264   under extreme viewing condition, GEMS simulations are limited to cloud fraction less than 0.5, SZAs

265 less than 60°, and fitting RMS (i.e., root mean square of fitting residuals relative to measurement errors)
266 less than 3.

267   Due to the different units of ozone amount between satellites and ozonesondes, we convert
268 ozonesonde-measured partial pressure ozone values (mPa) to partial column ozone (DU) at the 24
269 retrieval grids heights of the satellite for the altitude range from surface to the balloon-bursting altitudes.
270 Ozonesonde measurements are obtained at a rate of a few seconds and then typically averaged into
271 altitude increments of 100 meters, whereas retrieved ozone profiles from nadir BUV satellite
272 measurements have much coarser vertical resolution of 10-14 km in the troposphere and 7-11 km in the
273 stratosphere, based on OMI retrievals. Consequently, satellite observations capture only the smoothed
274 structures of ozonesonde soundings, especially near the tropopause, where a sharp vertical transition of
275 ozone within 1 km is observed, and in the boundary layer due to the insufficient penetration of photons.
276 Satellite retrievals unavoidably have an error compound due to its limited vertical resolution, called
277 "smoothing error" in OE-based retrievals (Rodgers, 2000). It could be useful to eliminate the effect of
278 smoothing errors on differences between satellites and sondes to better characterize other error sources
279 in comparisons (Liu et al., 2010a). For this reason, satellite data have been compared to ozonesonde
280 measurements smoothed to the satellite vertical resolution, together with original sonde soundings (Liu
281 et al., 2010b; Bak et al., 2013b; Huang et al., 2017). The smoothing approach is:

283        $\hat{x}_{sonde} = A \cdot x_{sonde} + (1 - A)x_a$ (3)
284   x_{sonde} : High-resolution ozonesonde profile
285              $\hat{x}_{sonde}$: Convolved ozonesonde profile into satellite vertical resolution
286   A   :   Satellite averaging kernel
287   x_a :   A priori ozone profile

289   In order to define tropospheric columns, both satellite retrievals and ozonesonde measurements
290 are vertically integrated from the surface to the tropopause taken from daily National Centers for
291 Environmental Prediction (NCEP) final (FNL) Operational Global analysis data
292 (http://rda.ucar.edu/datasets/ds083.2/). To account for the effect of surface height differences on
293 comparison, ozone amounts from satellite data below the surface heights of ozonesondes are added to
294 tropospheric columns of ozonesonde measurements and vice versa.

296 **3. Results and Discussions**

3.1 Comparison at individual stations

Witte et al. (2018) recently compared seven SHADOZ station ozonesonde records, including Hanoi and Kuala Lumpur in the GEMS domain, with total ozone and stratospheric ozone profiles measured by space-borne nadir and limb viewing instruments, respectively. In this comparison, the Hanoi station shows comparable or better agreement with the satellite datasets when compared to other sites. Morris et al. (2013) and Rohtash et al. (2016) thoroughly evaluated ozonesonde datasets over Japanese and Indian sites, respectively, but they did not address their measurement accuracy with respect to those at other stations. Validation of GOME TOC by Liu et al. (2006) showed relatively larger biases at Japanese CI stations and validation of OMI TOC by Huang et al. (2017) showed both larger biases and standard deviations at the India MBM sites. In South Korea, regular ozonesonde measurements are taken only from Pohang, but these measurements have been insufficiently evaluated; only the stratospheric parts of these measurements were quantitatively assessed against satellite solar occultation measurements by Halogen Occultation Experiment (HALOE) from 1995 to 2004 in Hwang et al. (2006), but only 26 pairs were compared despite the coarse coincident criteria (48 hours in time, $\pm 4.5^{\circ}$ in latitude, $\pm 9^{\circ}$ in longitude). Therefore, it is important to perform quality assessment of ozonesonde measurements to identify a reliable reference dataset for GEMS ozone profile validation

For this purpose, we illustrate tropospheric ozone columns (TOC) as a function of time for individual stations listed in Table 1, measured with three different types of ozonesonde instruments and retrieved with GEMS simulations (Fig. 5), respectively. The goal of this comparison is to identify any abnormal deviation of ozonesonde measurements relative to satellite retrievals, so we exclude the impact of the different vertical resolutions between instruments and satellite retrievals on this comparison by convolving ozonesonde data with satellite averaging kernels. At mid-latitude sites (Pohang, Sapporo, and Tsukuba) both ozonesonde and simulated retrievals show the distinct seasonal TOC variations with values ranging from ~ 35 to ~ 40 DU. Extratropical sites (Naha, Hong Kong, and Hanoi) show less seasonal variations, 30 to 50 DU, whereas fairly constant concentrations are observed at Kuala Lumpur and Singapore in the tropics. Both ozonesonde observations and simulated retrievals illustrate similar seasonal variabilities at these locations. At New Delhi and Trivandrum, on the other hand, MBM ozonesonde measurements abnormally deviate from 10 DU to 50 DU compared to the corresponding satellite retrievals and ozonesonde measurements at stations in similar latitudes.

In Fig. 6 time dependent errors in differences of TOC between ozonesonde and simulated GEMS retrievals are evaluated with the corresponding comparison statistics in Table 2. Simulated retrievals show strong correlation of ~ 0.8 or much larger with ozonesonde measurements at Pohang, Hong Kong, and three stations from Japan, and with less correlation of ~ 0.5 at other SHADOZ stations in the tropics.

However, Indian stations show poor correlation of 0.24. Mean biases and standard deviations are much smaller at stations where a strong correlation is observed; they are ~1 DU $\pm$~ 4DU at most ECC stations, but deviated to ~ 4 DU $\pm$~ 10 DU at MBM stations. In conclusion, we should exclude ozonesonde observations measured by MBM to remove irregularities in a reference dataset for validating both GEMS simulated retrievals in this study and GEMS actual retrievals in future study. Moreover, time series of ozonesonde and simulated retrievals show a significant transition at three Japanese stations as of late 2008 and early 2009 when the ozonesonde instruments were switched from CI to ECC. This transition could be affected by space-borne instrument degradation, but the impact of balloon-borne instrument change on them is predominant based on a less time-dependent degradation pattern at neighboring stations during this period. CI ozonesondes noticeably underestimate atmospheric ozone by 2-3 DU compared to ECC and thereby GEMS TOC biases relative to CI measurements are estimated as - 2 to - 5 DU, but these biases are reduced to < 1.5 DU when compared with ECC. Therefore, we decide to exclude these CI ozonesonde observations for evaluating GEMS simulated retrievals. Compared to other ECC stations, Hanoi Station often changed sensing solution concentrations and pH buffers (Table 1), which might cause the irregularities due to remaining errors even though transfer functions were applied to ozonesonde measurements to account for errors due to the different sensing solution (Witte et al., 2017). This fact might affect the relatively worse performance compared to a neighboring station, Hong Kong, where the 1.0 % KI buffered sensing solution (SST1.0) to ECC/SPC sensors have been consistently applied.

Fig. 7 compares differences of ozone profiles between ECC ozonesondes and GEMS simulated retrievals at each station. Among ECC ozonesondes, Singapore's are in the worst agreement with GEMS simulations in both terms of mean biases and standard deviations, which could be explained by the discrepancy in collocation time. Sonde observations at Japan, Pohang, Hong Kong, and Hanoi Stations, where balloons were launched in afternoon (~ 12-15 LT), are collocated within ~ 1-2 hours of OMI, whereas the time discrepancy increases to 7 hours at Singapore, where ozonesondes are launched in the early morning. Photochemical ozone concentrations are typically denser in the afternoon than in the morning and hence ozonesonde measurements at Singapore are negatively biased relative to afternoon satellite measurements. For the reason mentioned above, the discrepancy in the observation time could also affect this comparison at Kuala Lumpur, where sondes were mostly launched in the late morning, 2-3 hours prior to the OMI passing time and thereby ozonesonde measurements tend to be negatively biased. These indicate that diurnal variations of tropospheric ozone are visible in ozonesonde measurements, emphasizing the utility of hourly geostationary ozone measurements. The comparison results could be characterized with latitudes. In the mid-latitudes (Pohang, Tsukuba, and Sapporo),

365 noticeable disagreements are commonly seen in the tropopause region where mean biases/standard

366 deviations are ~10 %/~15% larger than those in the lower troposphere. In the extra-tropics (Hong Kong,

367 Naha), consistent differences of a few percent are seen over the entire altitude range with standard

368 deviations of 15 % or less below the tropopause (~ 15 km). Hanoi and Kuala Lumpur show significantly

369 larger biases/standard deviations compared to other ECC stations. At Hanoi inconsistencies of solution

370 concentrations and pH buffers might influence this instability. At Kuala Lumpur the inconsistencies of

371 observation times might be one of the reasons, considering its standard deviations of ~100 min, but

372 mostly less than 30 min at other stations. Therefore, we screen out Singapore, Kuala Lumpur, and Hanoi,

373 together with all MBM measurements at Indian stations and CI measurements at Japanese stations to

374 improve the validation accuracy of GEMS simulated retrievals in next section. Thus, stations where the

375 standard procedures for preparing and operating ECC sondes are consistently maintained, are adopted

376 as an optimal reference for this work.

377

378 **3.2 Evaluation of GEMS simulated ozone profile retrievals**

379

380   The GEMS simulated retrievals are assessed against ECC ozonesonde soundings at five stations

381 (Hong Kong, Pohang, Tsukuba, Sapporo, and Naha) identified as a good reference in the previous

382 section. The comparison statistics include mean bias and standard deviation in the absolute/relative

383 differences, correlation coefficients, linear regression results (slope (a), intercept (b), error); the error

384 of the linear regression is defined as $\frac{1}{n}\sqrt{\Sigma_i^n\left(y_{GEMS} - y_{fit}\right)^2}$, $y_{fit} = a \cdot y_{sonde} + b$. In Fig. 8, GEMS

385 simulated retrievals are plotted as functions of ozonesondes with and without the vertical resolution

386 smoothing, respectively, for the stratospheric and tropospheric columns. GEMS simulations

387 underestimate the tropospheric ozone by ~ 2.27 $\pm$ 5.94 DU and overestimate the stratospheric ozone

388 by ~ 9.35 $\pm$ 8.07 DU relative to high-resolution ozonesonde observations. This comparison

389 demonstrates good correlation coefficients of 0.84 and 0.99 for troposphere and stratosphere,

390 respectively. This agreement is degraded if the rejected ECC sondes (Kuala Lumpur, Hanoi, and

391 Singapore) are included; for example, the slope decreases from 0.68 to 0.64 while the RMSE increases

392 6.35 and 6.76 DU for TOC comparison. Smoothing ozonesonde soundings to GEMS vertical resolution

393 improves the comparison results, especially for the tropospheric ozone columns; standard deviations

394 are reduced by ~ 5 % with mean biases of less than 1 DU. Similar assessments are performed for OMI

395 standard ozone profiles based on the KNMI OE algorithm (Kroon et al., 2011) hereafter referred to as

396 OMO3PR (KNMI) in Fig. 9 and the research product based on the SAO algorithm (Liu et al., 2010)

397 hereafter referred to as OMPROFOZ (SAO) in Fig. 10, respectively. It implies that GEMS gives good

information on Stratospheric Ozone Columns (SOCs) comparable to both the OMI KNMI and SAO products in spite of insufficient information on Hartley ozone absorption in GEMS. Furthermore, a better agreement of GEMS TOCs with ozonesonde is found than with the others due to different implementation details. As mentioned in 2.1., the GEMS algorithm is developed based on the heritages of the SAO ozone profile algorithm with several modifications. The two main modifications are: (1) a priori ozone climatology was replaced with a tropopause-based ozone profile climatology to better represent the ozone variability in the tropopause (2) irradiance spectra used to normalize radiance spectra and characterize instrument line shapes are prepared by taking 31-day moving average instead of climatological average to take into account for time-dependent instrument degradation. These modifications reduce somewhat the spread in deviations of satellite retrievals from sondes, especially in TOC comparison. KNMI retrievals systematically overestimate the tropospheric ozone by ~ 6 DU (Fig. 10.c), which corresponds to the positive biases of 2-4 % in the integrated total columns of KNMI profiles relative to Brewer observations (Bak et al., 2015). As mentioned in Bak et al. (2015), the systematic biases in ozone retrievals are less visible in SAO-based retrievals (simulated GEMS data, OMPROFOZ), as systematic components of measured spectra are taken into account for using an empirical correction called "soft calibration".

4. Summary

We simulate GEMS ozone profile retrievals from OMI BUV radiances in the range 300-330 nm using the OE-based fitting during the period 2005-2015 to ensure the performance of the algorithm against coincident ozonesonde observations. There are 10 ozonesonde sites over the GEMS domain from WOUDC, SHADOZ and KMA archives. This paper gives an overview of these ozonesonde observation systems to address inhomogeneities in preparation, operation, and correction procedures which cause discontinuities in individual long-term records or among stations. Comparisons between simulated GEMS TOCs and ozonesondes illustrate a noticeable dependence on the instrument type. Indian ozonesonde soundings measured by MBM show severe deviations in seasonal time series of TOC compared to coherent GEMS simulations and ozonesonde observations measured in similar latitude regime. At Japanese stations, CI ozonesondes underestimate ECC ozonesondes by 2 DU or more and a better agreement with GEMS simulations is found when ECC measurements are compared. Therefore, only ECC ozonesonde measurements are selected as a reference, in order to ensure a consistent, homogeneous dataset. Furthermore, ECC measurements at Singapore, Kuala Lumpur, and Hanoi are excluded. At Singapore and Kuala Lumpur, observations were performed in the morning and thereby are inconsistent with GEMS retrievals simulated at the OMI overpass time in the afternoon. In

432 addition, the observation time for Kuala Lumpur is inconsistent itself compared to other stations; its
433 standard deviation is ~ 100 min, but for other ECC stations it is less than 30 min. At Hanoi the
434 combinations of sensing solution concentrations and pH buffers changed 4 times during the period of
435 2005 through 2015. Therefore, GEMS and ozonesonde comparisons show larger biases/standard
436 deviations at these stations. Pohang station is unique in South Korea where ECC ozonesondes have
437 been regularly and consistently launched without a gap since 1995; the standard 1% KI full buffered
438 sensing solution has been consistently applied to ozone sensors manufactured by SPC (6A model).
439 Evaluation of Pohang ozonesondes against GEMS simulations demonstrates its high level reliability,
440 which is comparable to neighboring Japanese ECC measurements at Tsukuba and Sapporo. Reasonable
441 agreement with GEMS simulated retrievals is similarly shown at adjacent Naha and Hong Kong stations.
442 Finally, we establish that the comparison statistics of GEMS simulated retrievals and optimal reference
443 dataset is -2.27 (4.92) $\pm$ 5.94 (14.86) DU (%) with R = 0.84 for the tropospheric columns and 9.35
444 (5.09) $\pm$ 8.07 (4.60) DU (%) with R=0.99 for the stratospheric columns. This estimated accuracy and
445 precision is comparable to OMI products for the stratospheric ozone column and even better for the
446 tropospheric ozone column due to improved algorithm implementation. Our future study aims to
447 achieve this quality level from actual GEMS ozone profile product.
448
449 *Author contributions.* JB and KHB designed the research; JHK and JK provided oversight and
450 guidance; JB conducted the research and wrote the paper; XL and KC contributed to the
451 analysis and writing.

452 *Competing interests.* The authors declare that they have no conflict of interest.

453
454 *Data availability*, The ozonesonde data used in this study were obtained though the WOUDC,
455 SHADOZ and KMA archives. The WOUDC dataset are available at
456 https://woudc.org/data/products/ozonesonde/(last access: 07 July 2019) and for the SHADOZ dataset
457 at https://tropo.gsfc.nasa.gov/shadoz/Archive.html (last access:07 July 2019). The KMA dataset is
458 available through data request at https://www.data.go.kr/. OMI Level1b radiane dataset are available at
459 https://aura.gesdisc.eosdis.nasa.gov/data///Aura_OMI_Level1/ (last access:07 July 2019).

460 *Acknowledgement,* Research at the Smithsonian Astrophysical Observatory was funded by NASA and
461 the Smithsonian Institution. Research at Pusan National University was supported by Basic Science
462 Research Program through the National Research Foundation of Korea (NRF) funded by the Ministry
463 of Education (2016R1D1A1B01016565). This work was also supported by the Korea Ministry of
464 Environment (MOE) as the Public Technology Program based on Environmental Policy
465 (2017000160001). *Financial support.* This research has been supported by the Korea Ministry of

466 Environment (MOE) as the Public Technology Program based on Environmental Policy
467 (2017000160001)
468

469   **Reference**

470 Bak, J., Kim, J. H., Liu, X., Chance, K., and Kim, J.: Evaluation of ozone profile and tropospheric ozone retrievals
471   from GEMS and OMI spectra, Atmos. Meas. Tech., 6, 239-249, doi:10.5194/amt-6-239-2013, 2013a.

472 Bak, J., Liu, X., Wei, J. C., Pan, L. L., Chance, K., and Kim, J. H.: Improvement of OMI ozone profile retrievals
473   in the upper troposphere and lower stratosphere by the use of a tropopause-based ozone profile climatology,
474   Atmos. Meas. Tech., 6, 2239–2254, doi:10.5194/amt-6-2239-2013, 2013b.

475 Bak, J., Liu, X., Kim, J.-H., Haffner, D. P., Chance, K., Yang, K., and Sun, K.: Characterization and correction of
476   OMPS nadir mapper measurements for ozone profile retrievals, Atmos. Meas. Tech., 10, 4373-4388,
477   https://doi.org/10.5194/amt-10-4373-2017, 2017.

478 Bhartia, P. K., McPeters, R. D., Mateer, C. L., Flynn, L. E., and Wellemeyer, C.: Algorithm for the estimation of
479   vertical ozone profiles from the backscattered ultraviolet technique, J. Geophys. Res., 101, 18793–18806,
480   1996.

481 Bovensmann, H., Burrows, J. P., Buchwitz, M., Frerick, J., Noel, S., Rozanov, V. V., Chance, K. V., and Goede,
482   A. P. H.: SCIAMACHY: Mission objectives and measurement modes, J. Atmos. Sci., 56, 127–150,
483   doi:10.1175/1520-0469(1999)056<0127:SMOAMM>2.0.CO;2, 1999.

484 Cai, Z., Liu, Y., Liu, X., Chance, K., Nowlan, C. R., Lang, R., Munro, R., and Suleiman, R.: , Characterization
485   and correction of Global Ozone Monitoring Experiment 2 ultraviolet measurements and application to ozone
486   profile retrievals, J. Geophys. Res., 117, D07305, doi: 10.1029/2011JD017096, 2012.

487 Chance, K., Liu, X., Suleiman, R. M., Flittner, D. E., Al-Saadi, J., and Janz, S. J.: Tropospheric emissions:
488   monitoring of pollution (TEMPO), Proc. SPIE 8866, Earth Observing Systems XVIII, 8866, 88660D-1–
489   88660D-16, doi:10.1117/12.2024479, 2013.

490 Deshler, T., Stübi, R., Schmidlin, F. J., Mercer, J. L., Smit, H. G. J., Johnson, B. J., Kivi, R., and Nardi, B.: Methods
491   to homogenize electrochemical concentration cell (ECC) ozonesonde measurements across changes in sensing
492   solution concentration or ozonesonde manufacturer, Atmos. Meas. Tech., 10, 2021-2043,
493   https://doi.org/10.5194/amt-10-2021-2017, 2017.

494 European Space Agency: The GOME Users Manual, ESA Publ. SP-1182, Publ. Div., Eur. 488 Space Res. and
495   Technol. Cent., Noordwijk, The Netherlands, 1995.

496 European Organization for the Exploitation of Meteorological Satellites (EUMETSAT): GOME-2 level 1 Product
497   Generation Specification, Rep. EPS.SYS.SPE.990011, Darmstadt, Germany, 2006.

498 Fioletov, V. E., Labow, G., Evans, R., Hare, E. W., Khler, U., McElroy, C. T., Miyagawa, K., Redondas, A.,
499   Savastiouk., V., Shalamyansky, A. M., Staehelin, J., Vanicek, K., and Weber, M.: Performance of the ground-
500   based total ozone network assessed using satellite data, J. Geophys. Res., 113, D14313, doi:
501   10.1029/2008JD009809, 2008.

502 Flynn, L., Long, C., Wu, X., Evans, R., Beck, C. T., Petropavlovskikh, I., McConville, G., Yu, W., Zhang, Z., Niu,

J., Beach, E., Hao, Y., Pan, C., Sen, B., Novicki, M., Zhou, S., and Seftor, C. : Performance of the Ozone Mapping and Profiler Suite (OMPS) products, J. Geophys. Res. Atmos., 119, 6181–6195, doi: 10.1002/2013JD020467, 2014.

Hwang, S.-H., J. Kim, J., and Cho, G.-R., Observation of secondary ozone peaks near the tropopause over the Korean peninsula associated with stratosphere-troposphere exchange, J. Geophys. Res., 112, D16305, doi: 10.1029/2006JD007978, 2007.

Huang, G., Liu, X., Chance, K, Yang et al. : Validation of 10-year SAO OMI Ozone Profile (PROFOZ) Product Using Ozonesonde Observations, Atmos. Meas. Tech. Discuss., doi: 10.5194/amt-2017-15, 2017.

Ingmann, P., Veihelmann, B., Langen, J., Lamarre, D., Stark, H., and Courrèges-Lacoste, G. B.: Requirements for the GMES atmosphere service and ESA's implementation concept: Sentinels-4/-5 and-5p, Remote Sens. Environ., 120, 58–69, doi:10.1016/j.rse.2012.01.023, 2012.

Kroon, M., de Haan, J. F., Veefkind, J. P., Froidevaux, L., Wang, R., Kivi, R., and Hakkarainen, J. J.: Validation of operational ozone profiles from the Ozone Monitoring Instrument, J. Geophys. Res., 116, D18305, doi: 10.1029/2010JD015100, 2011.

Lal, S., Naja, M., and Subbaraya, B: Seasonal variations in surface ozone and its precursors over an urban site in India, Atmospheric Environment, Volume 34, Issue 17, 2000, Pages 2713-2724, 2000.

Levelt, P. F., van den Oord, G. H. J., Dobber, M. R., Malkki, A., Visser, H., de Vries, J., Stammes, P., Lundell, J. O. V., and Saari, H.: The Ozone Monitoring Instrument, IEEE Trans. Geosci. Remote Sens., 44(5), 1093–1101, doi:10.1109/TGRS.2006.872333, 2006.

Liu, H., D. J. Jacob, L. Y. Chan, S. J. Oltmans, I. Bey, R. M. Yantosca, J. M. Harris, B. N. Duncan, and R. V. Martin, Sources of tropospheric ozone along the Asian Pacific Rim: An analysis of ozonesonde observations, J. Geophys. Res., 107(D21), 4573, doi:10.1029/2001JD002005, 2002.

Liu, X., Chance, K., Sioris, C. E., Spurr, R. J. D., Kurosu, T. P., Martin, R. V., and Newchurch, M. J.: Ozone profile and tropospheric ozone retrievals from Global Ozone Monitoring Experiment: algorithm description and validation, J. Geophys. Res., 110, D20307, doi: 10.1029/2005JD006240, 2005.

Liu, X., Chance, K., Sioris, C. E., Kurosu, T. P., and Newchurch, M. J. : Intercomparison of GOME, ozonesonde, and SAGE II measurements of ozone: Demonstration of the need to homogenize available ozonesonde data sets, J. Geophys. Res., 111, D14305, doi:10.1029/2005JD006718, 2006.

Liu, X., Bhartia, P.K, Chance, K, Spurr, R.J.D., and Kurosu, T.P.: Ozone profile retrievals from the ozone monitoring instrument. Atmos. Chem. Phys., 10, 2521–2537, 2010a.

Liu, X., Bhartia, P. K., Chance, K., Froidevaux, L., Spurr, R. J. D., and Kurosu, T. P.: Validation of Ozone Monitoring Instrument (OMI) ozone profiles and stratospheric ozone columns with Microwave Limb Sounder (MLS) measurements, Atmos. Chem. Phys., 10, 2539–2549, doi:10.5194/acp-10-2539-2010, 2010b.

Morris, G. A., Labow, G., Akimoto, H., Takigawa, M., Fujiwara, M., Hasebe, F., Hirokawa, J., and Koide, T.: On the use of the correction factor with Japanese ozonesonde data, Atmos. Chem. Phys., 13, 1243-1260, https://doi.org/10.5194/acp-13-1243-2013, 2013.

Ogino, S.-Y., M. Fujiwara, M. Shiotani, F. Hasebe, J. Matsumoto, T. H. T. Hoang, and T. T. T. Nguyen (2013),

540
541 Ozone variations over the northern subtropical region revealed by ozonesonde observations in Hanoi, J. Geophys. Res. Atmos., 118, 3245–3257, doi:10.1002/jgrd.50348.

Petropavlovskikh, I., Evans, R., McConville, G., Oltmans, S., Quincy, D., Lantz, K., Disterhoft, P., Stanek, M., and Flynn, L.: Sensitivity of Dobson and Brewer Umkehr ozone profile retrievals to ozone cross-sections and stray light effects, Atmos. Meas. Tech., 4, 1841–1853, doi:10.5194/amt-4-1841-2011, 2011.

Rodgers, C. D.: Inverse Methods for Atmospheric Sounding: Theory and Practice, World Scientific Publishing, Singapore, 2000.

Rohtash, Mandal, T.K., Peshin, S.K. S. K. Peshin and Sharma1, S. K., Study on Comparison of Indian Ozonesonde Data with Satellite Data, MAPAN-Journal of Metrology Society of India 31: 197.doi:10.1007/s12647-016-0174-4, 2016.

Schenkeveld, V. M. E., Jaross, G., Marchenko, S., Haffner, D., Kleipool, Q. L., Rozemeijer, N. C., Veefkind, J. P., and Levelt, P. F.: In-flight performance of the Ozone Monitoring Instrument, Atmos. Meas. Tech., 10, 1957-1986, https://doi.org/10.5194/amt-10-1957-2017, 2017.

Smit, H. G. J., Straeter, W., Johnson, B., Oltmans, S., Davies, J., Tarasick, D. W., Hoegger, B., Stubi, R., Schmidlin, F., Northam, T., Thompson, A., Witte, J., Boyd, I., and Posny, F.: Assessment of the performance of ECC-ozonesondes under quasi-flight conditions in the 10 environmental simulation chamber: Insights from the Juelich Ozone Sonde Intercomparison Experiment (JOSIE), J. Geophys. Res., 112, D19306, doi: 10.1029/2006JD007308, 2007.

Smit,, H. G. J., and the Panel for the Assessment of Standard Operating Procedures for Ozonesondes (ASOPOS) : Guidelines for homogenization of ozonesonde data, SI2N/O3S-DQA activity as part of "Past changes in the vertical distribution of ozone assessment". [Available at http://www-das.uwyo.edu/%7Edeshler/NDACC_O3Sondes/O3s_DQA/O3S-DQA-Guidelines%20Homogenization-V2-19November2012.pdf.], 2012.

Sun, K., Liu, X., Huang, G., Gonzalez Abad, G, Cai, Z., Chance, K., and Yang, K. : Deriving the slit functions from OMI solar observations and its implications for ozone-profile retrieval, Atmos. Meas. Tech., 10, 3677-3695, https://doi.org/10.5194/amt-10-3677-2017, 2017.

Spurr, R. J.: VLIDORT: A linearized pseudo-spherical vector discrete ordinate radiative transfer code for forward model and retrieval studies in multilayer multiple scattering media, J. Quant. Spectrosc. Ra., 102, 316–342, doi:10.1016/j.jqsrt.2006.05.005, 2006.

Spurr, R. J. D.: Linearized pseudo-spherical scalar and vector discrete ordinate radiative transfer models for use in remote sensing retrieval problems, in: Light Scattering Reviews, edited by: Kokhanovsky, A., Springer, New York, 2008.

Veefkind, J. P., Aben, I., McMullan, K., Förster, H., de Vries, J., Otter, G., Claas, J., Eskes, H. J., de Haan, J. F., Kleipool, Q., van Weele, M., Hasekamp, O., Hoogeveen, R., Landgraf, J., Snel, R., Tol, P., Ingmann, P., Voors, R., Kruizinga, B., Vink, R., Visser, H. and Levelt, P. F.: TROPOMI on the ESA Sentinel-5 Precursor: A GMES mission for global observations of the atmospheric composition for climate, air quality and ozone layer applications, Remote Sensing of Environment, 120(0), 70–83, doi:10.1016/j.rse.2011.09.027, 2012.

Thompson, A. M., Stone, J. B., Witte, J. C., Miller, S. K., Oltmans, S. J., Kucsera, T. L., Ross, K. L., Pickering, K. E., Merrill, J. T., Forbes, G., Tarasick, D. W., Joseph, E., Schmidlin, F. J., McMillan, W.W.,Warner, J., Hintsa, E. J., and Johnson, J. E.: Intercontinental Chemical Transport Experiment Ozonesonde Network Study (IONS) 2004: 2. Tropospheric ozone budgets and variability over northeastern North America, J. Geophys. Res., 112, D12S13, doi:10.1029/2006JD007670, 2007.

Thompson, A. M., Witte, J. C., Sterling, C., Jordan, A., Johnson, B. J., Oltmans, S. J., Fujiwara, M. Vömel, H. Allaart, M., Piters, A., Coetzee, J. G. R., Posny, F., Corrales, E., Andres Diaz, J., Félix, C., Komala, N., Lai, N. Maata, M., Mani, F., Zainal, Z., Ogino, S-Y., Paredes, F., Bezerra Penha, T. L., Raimundo da Silva, F., Sallons-Mitro, S., Selkirk, H. B., Schmidlin, F. J., Stuebi, R., and Thiongo, K.: First reprocessing of Southern Hemisphere Additional Ozonesondes (SHADOZ) Ozone Profiles (1998-2016). 2. Comparisons with satellites and ground-based instruments, J. Geophys. Res., JD027406, https://doi.org/10.1002/2017JD027406, 2017.

WMO: Scientific Assessment of Ozone Depletion: 2014, Global Ozone Research and Monitoring Project-Report No. 55, 416 pp., Geneva, Switzerland, 2014.

Witte J.C., Thompson A.M., Smit H.G.J., Fujiwara M., Posny F., Coetzee G.J.R., Northam E.T., Johnson B.J., Sterling C.W., Mohamad M., Ogino S.- Y., Jordan A., da Silva F.R.: First reprocessing of Southern Hemisphere Additional OZonesondes (SHADOZ) profile records (1998–2015): 1. Methodology and evaluation, J. Geophys. Res. Atmos., 122, 6,611-6,636, 2017.

Witte J.C., Thompson A.M., Smit H.G.J., Vömel H., Posny F., Stübi R.: First reprocessing of Southern Hemisphere Additional OZonesondes profile records: 3. Uncertainty in ozone profile and total column. J. Geophys. Res. Atmos., 123, 2018.

Zoogman, P., Liu, X., Suleiman, R. M., Pennington, W. F., Flittner, D. E., Al-Saadi, J. A., Hilton, B. B., Nicks, D. K., Newchurch, M. J., Carr, J. L., Janz, S. J., Andraschko, M. R., Arola, A., Baker, B. D., Canova, B. P., Chan Miller, C., Cohen, R. C., Davis, J. E., Dussault, M. E., Edwards, D. P., Fishman, J., Ghulam, A., González Abad, G., Grutter, M., Herman, J. R., Houck, J., Jacob, D. J., Joiner, J., Kerridge, B. J., Kim, J., Krotkov, N. A., Lamsal, L., Li, C., Lindfors, A., Martin, R. V., McElroy, C. T., McLinden, C., Natraj, V., Neil, D. O., Nowlan, C. R., O'Sullivan, E. J., Palmer, P. I., Pierce, R. B., Pippin, M. R., Saiz-Lopez, A., Spurr, R. J. D., Szykman, J. J., Torres, O., Veefkindz, J. P., Veihelmann, B.,Wang, H.,Wang, J., and Chance, K.: Tropospheric Emissions: Monitoring of Pollution (TEMPO), J. Quant. Spectrosc. Ra., 186, 17–39, https://doi.org/10.1016/j.jqsrt.2016.05.008, 2017.
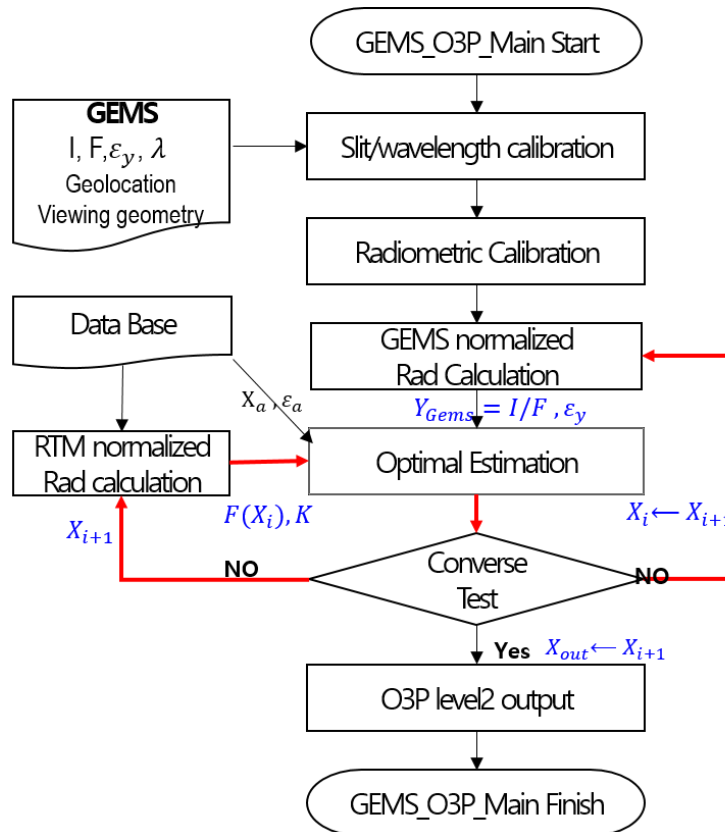
Figure 1. Flow chart of the GEMS ozone profile retrieval algorithm.
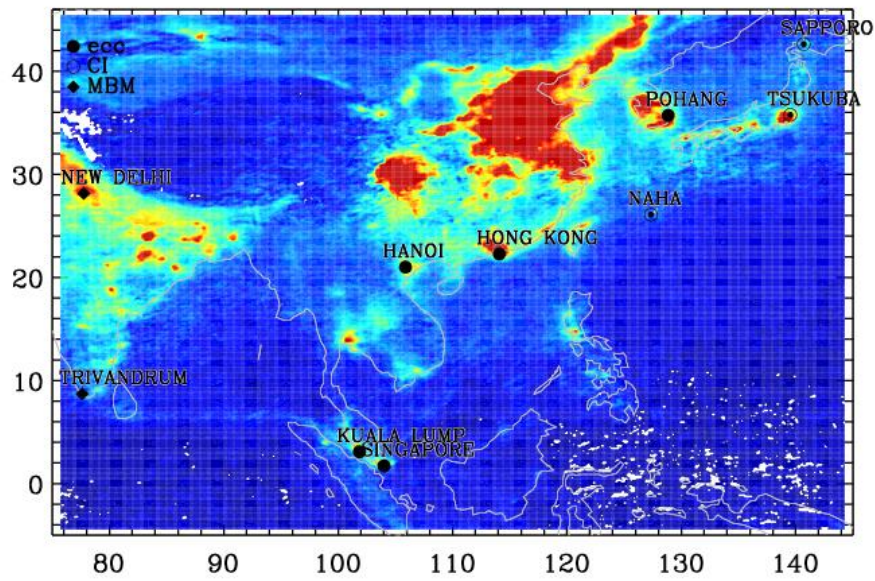
Figure 2. Geographic locations of the ozonesonde stations available since 2005 over the GEMS observation domain. Each symbol represents a different type sensor; the modified Brewer-Mast (MBM), the carbon iodine cell (CI), and the electrochemical concentration cell (ECC). The background map illustrates the OMI NO$_2$ monthly mean in June 2015.
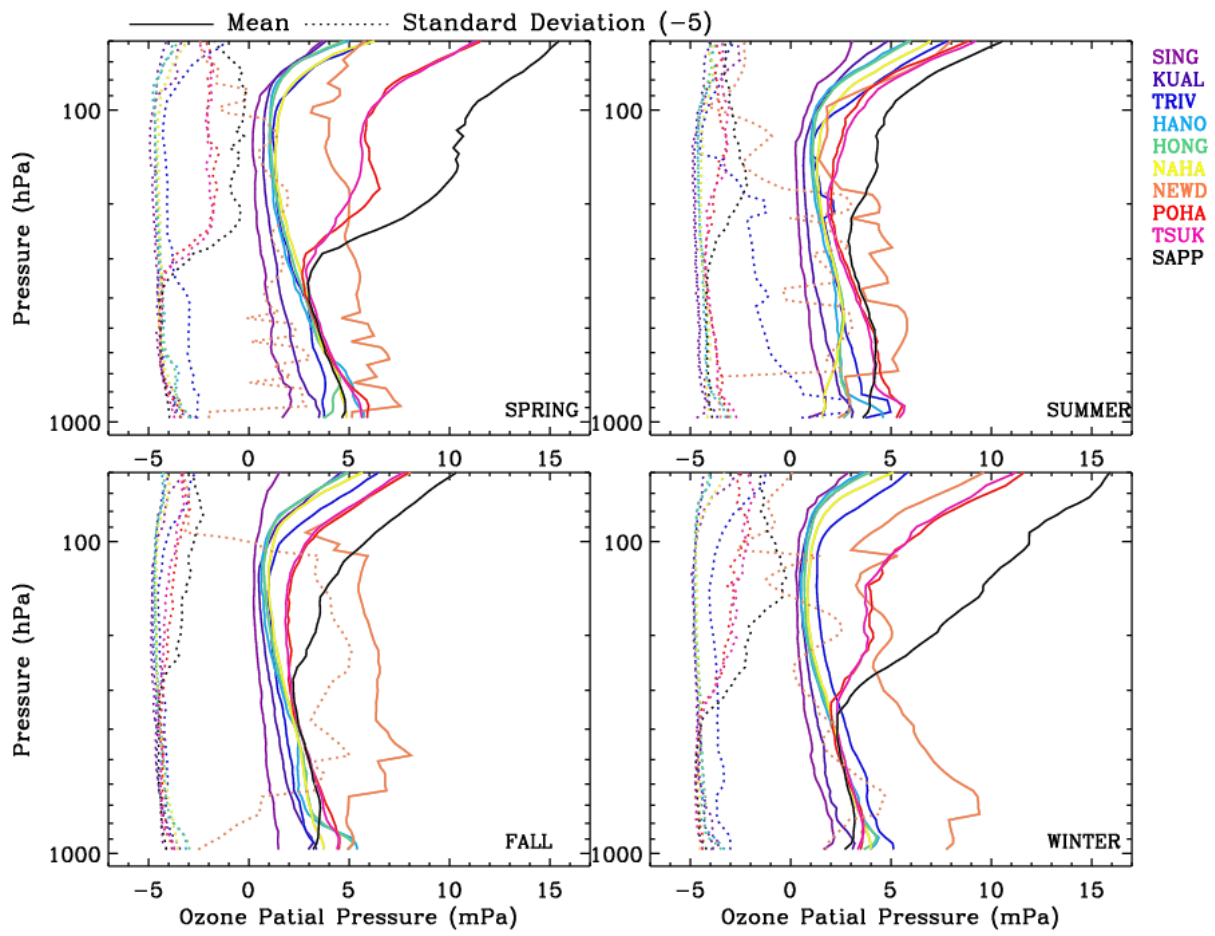
Figure 3. Seasonal mean (solid) and standard deviation (dashed) profiles of ozonesonde soundings from 2005 to 2015 at the 10 sites listed in Table 1. 5 mPa is subtracted from standard deviations to fit the x-axis.
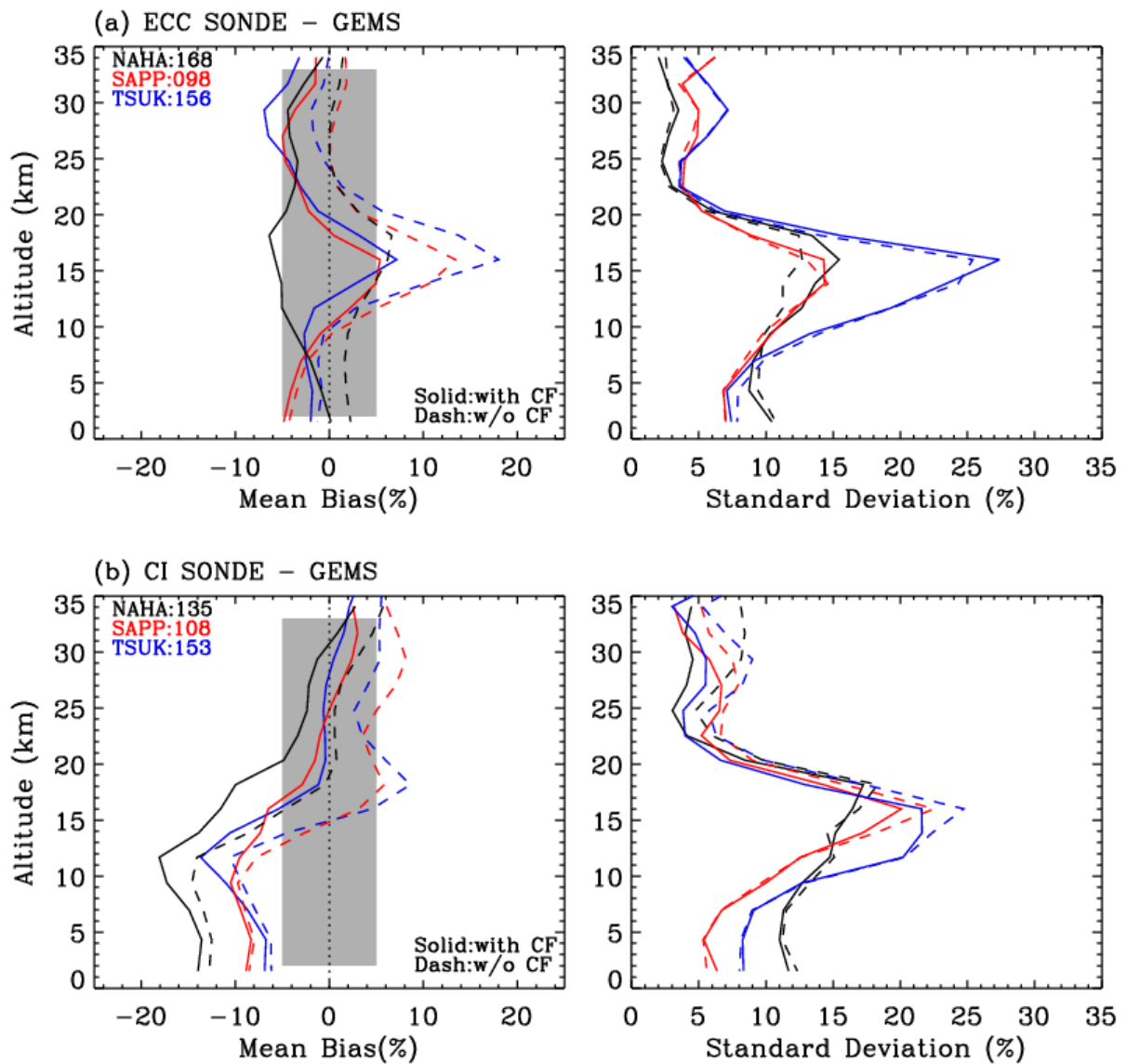
Figure 4. Effects of applying a correction factor (CF) to (a) ECC and (b) CI ozonesonde measurements, respectively, on comparisons with simulated GEMS ozone profile retrievals. Solid and dashed lines represent the comparisons with and without applying a CF, respectively, at each Japanese station. The number of data point is included in the legends.
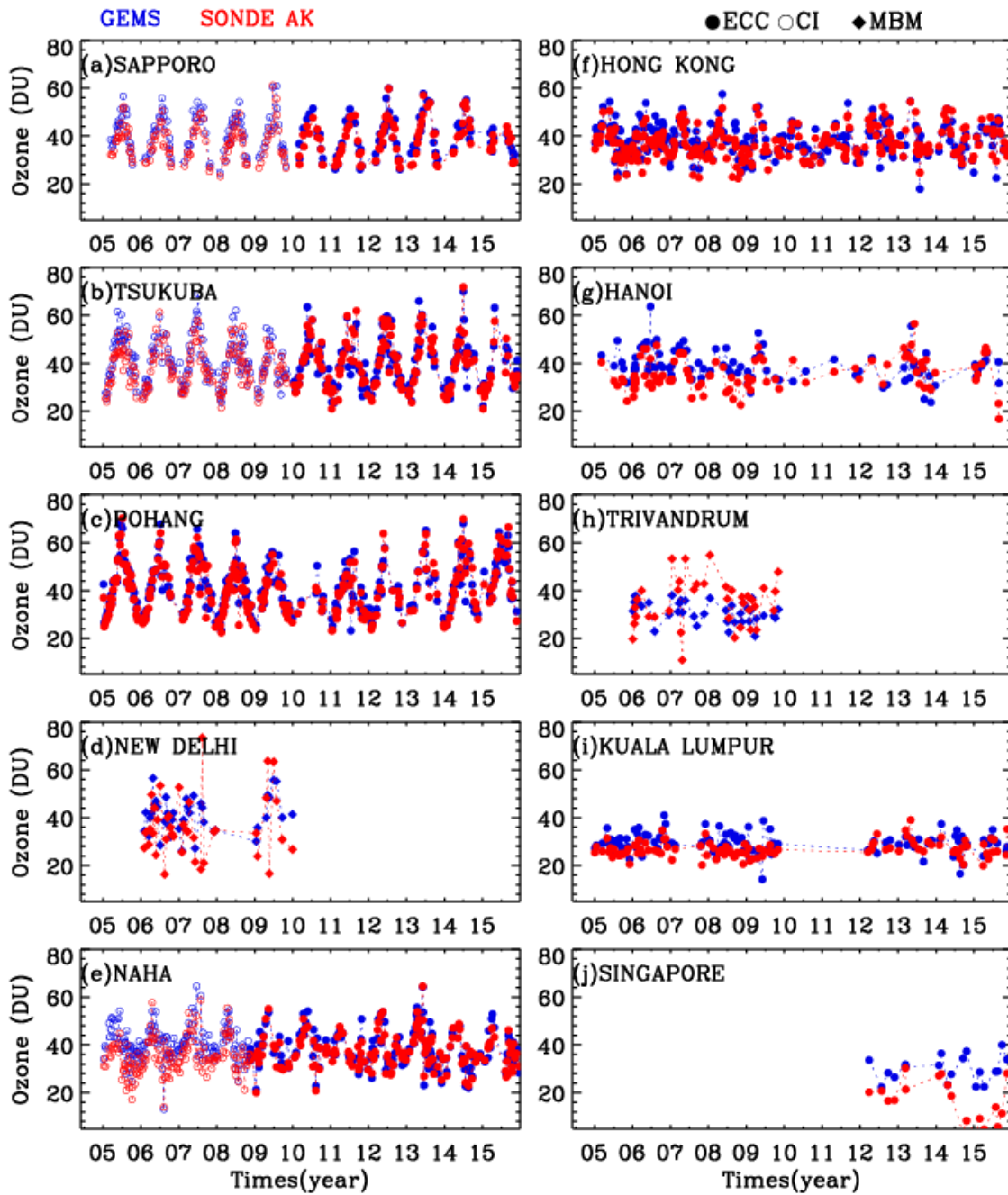
Figure 5. Time series of tropospheric ozone columns (DU) of GEMS simulated ozone profile retrievals (blue) and ozonesonde measurements convolved with GEMS averaging kernels (red) from 2005 to 2015 at 10 stations listed in Table 1.
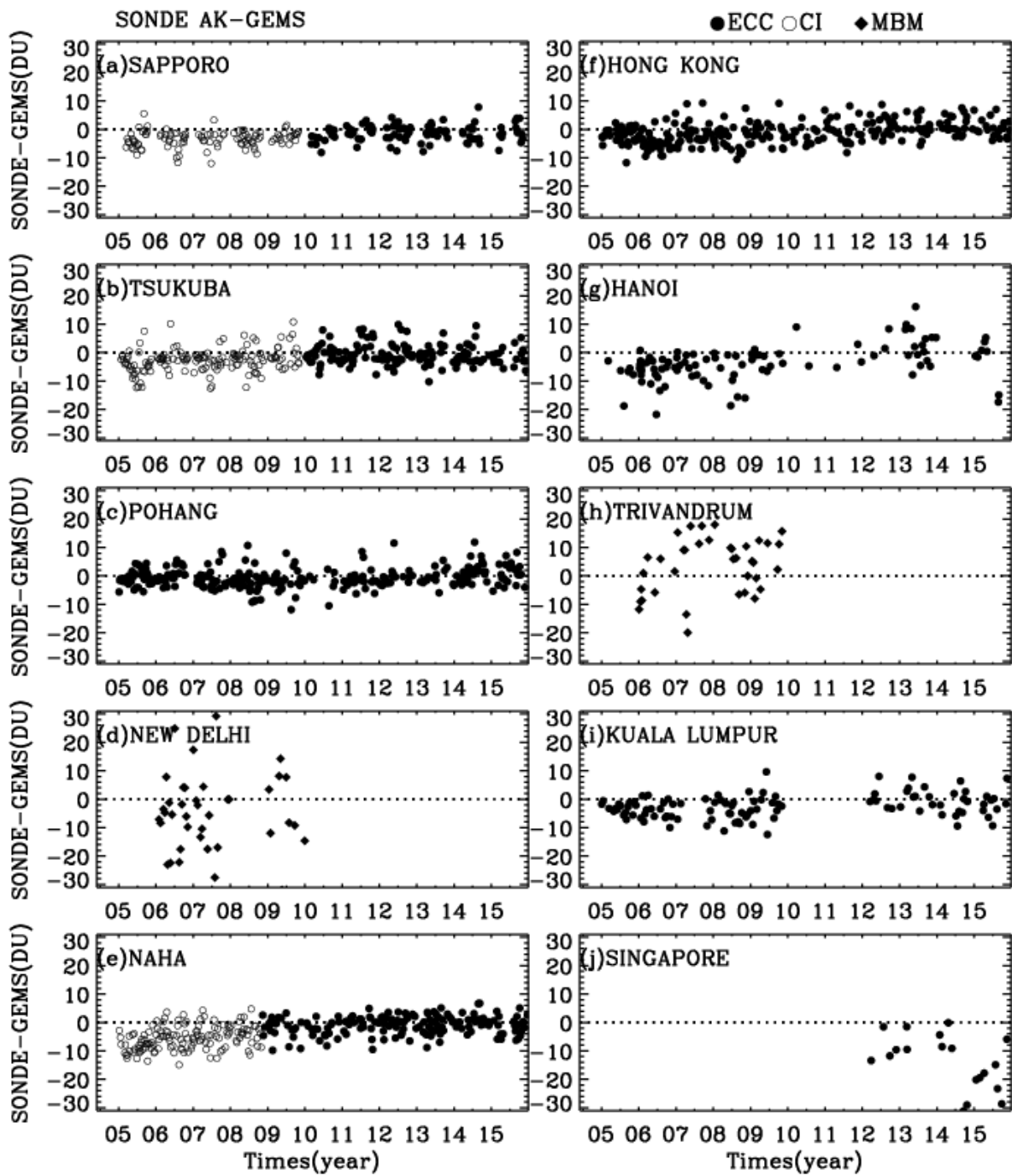
Figure 6. Same as Figure 5, but for absolute differences of tropospheric ozone columns (DU) between ozonesonde measurements and GEMS simulated retrievals.
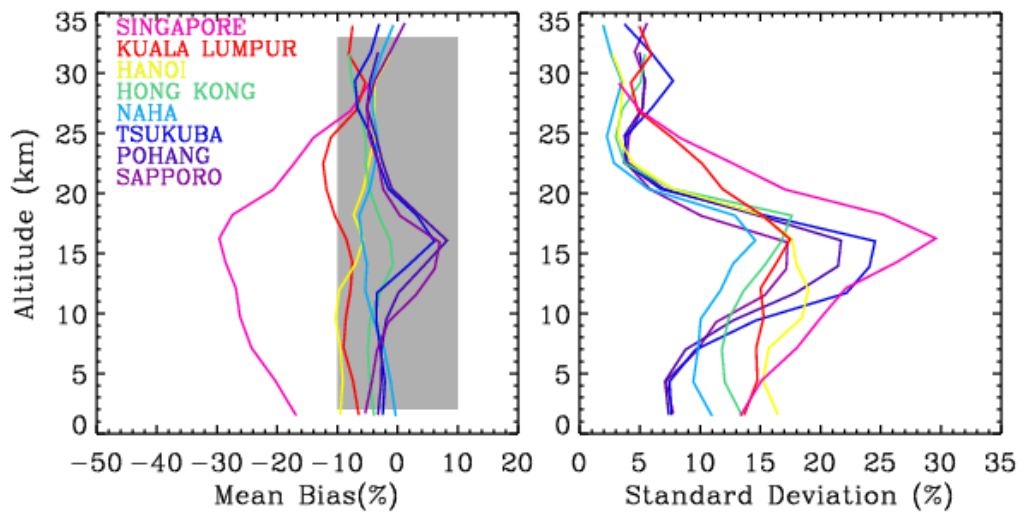
Figure 7. Mean biases and 1σ standard deviations of the differences between ozonesonde convolved with GEMS averaging kernels and GEMS simulated ozone retrievals as a function of GEMS layers, at individual ECC ozonesonde stations. The relative difference is defined as   (SONDE AK – GEMS) ×100 %/ (a priori).
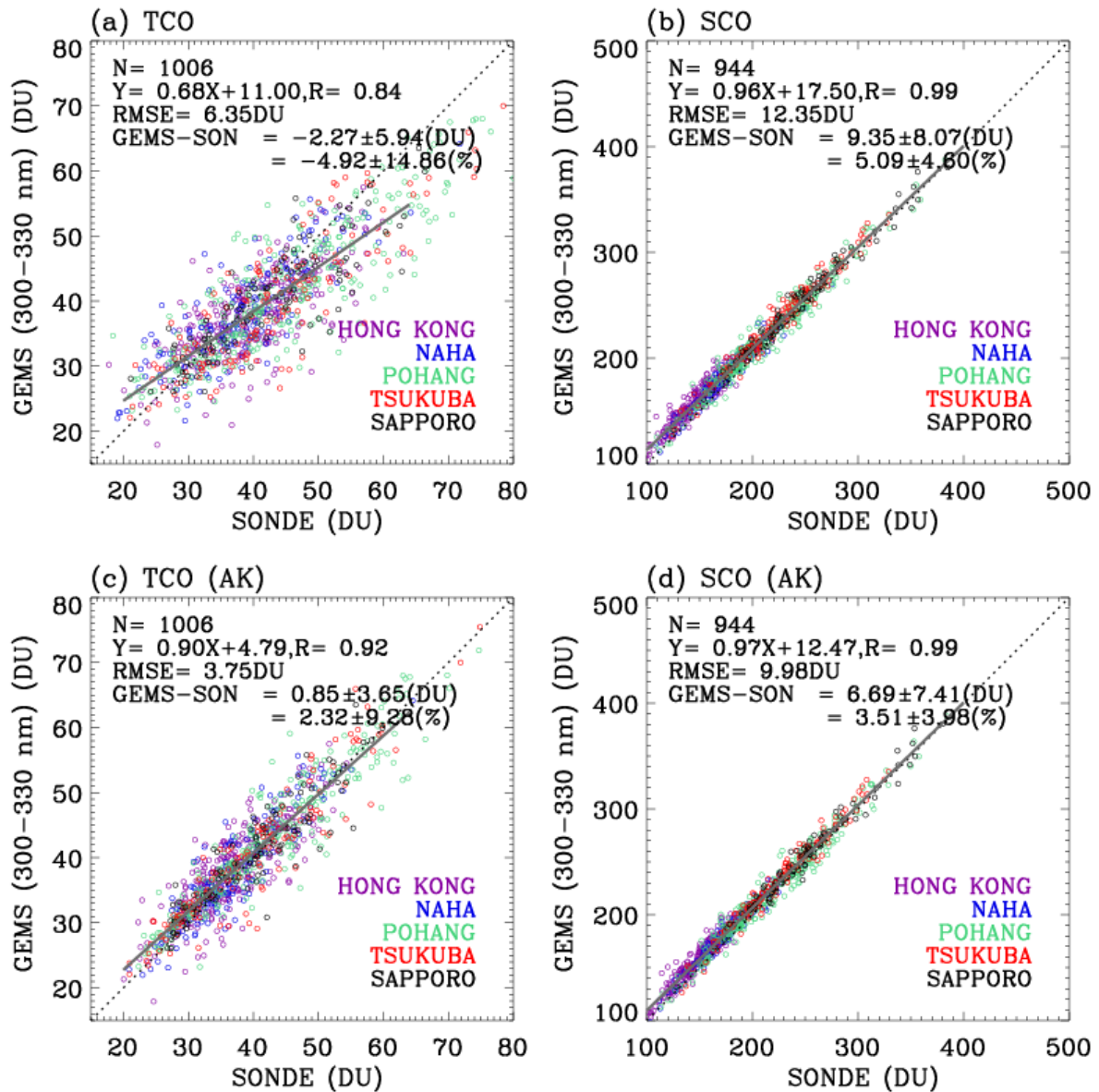
Figure 8. Upper: Scatter plots of GEMS vs. ozonesonde for tropospheric and stratospheric ozone columns, respectively. The lower panels are the same as the upper ones, except that ozonesonde measurements are convolved with GEMS averaging kernels. A linear fit between them is shown in red, with the 1:1 lines (dotted lines). The legends show the number of data points (N), the slope and intercept of a linear regression, and correlation coefficient (r), with mean biases and 1σ standard deviations for absolute (DU) and relative differences (%), respectively. Note that we use 5 stations identified as a good reference among 10 stations listed in Table 1 in this comparison.
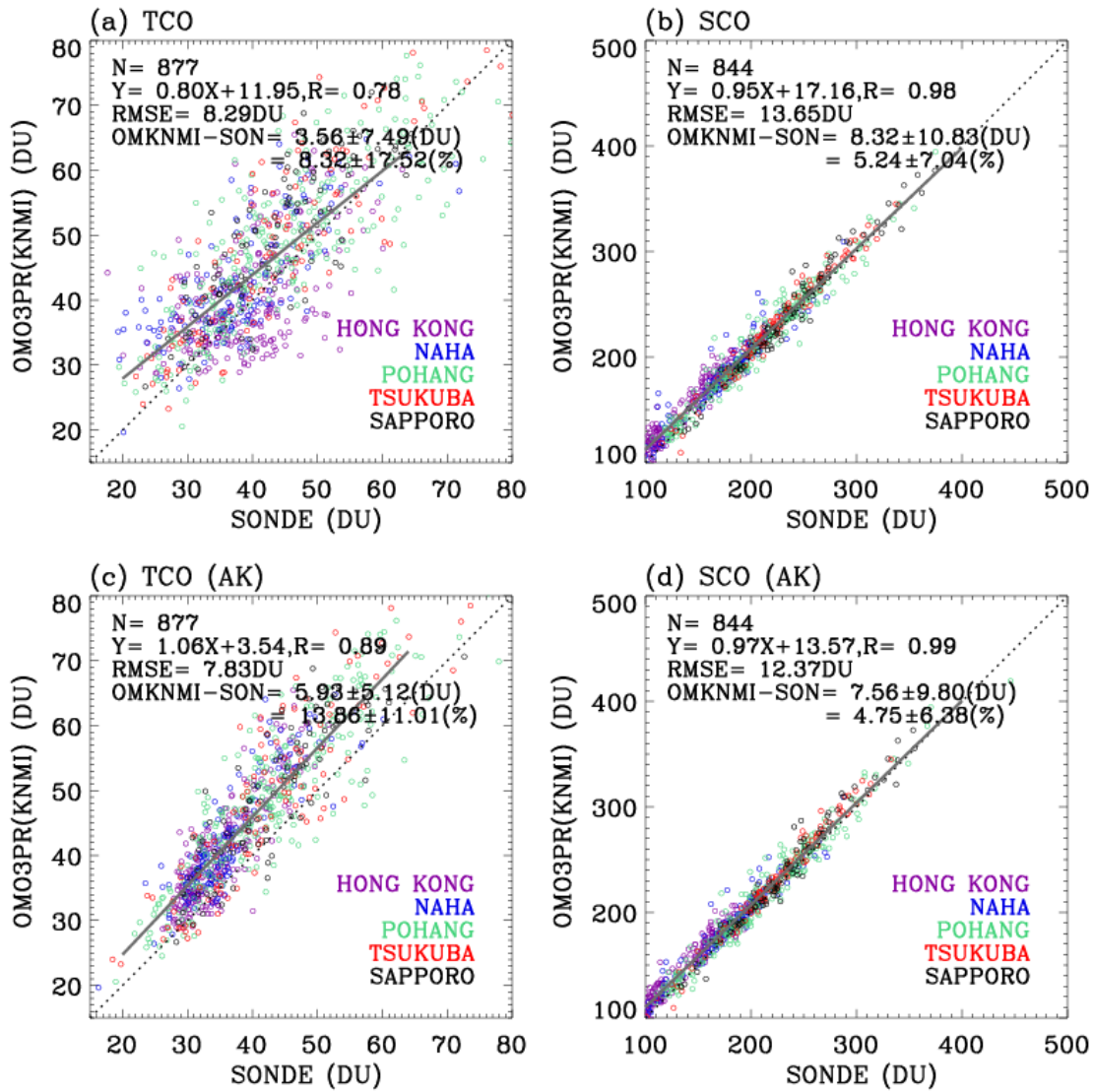
Figure 9. Same as Fig. 8, but for validating OMI standard ozone profiles (OMO3PR) produced by the KNMI OE-based algorithm.
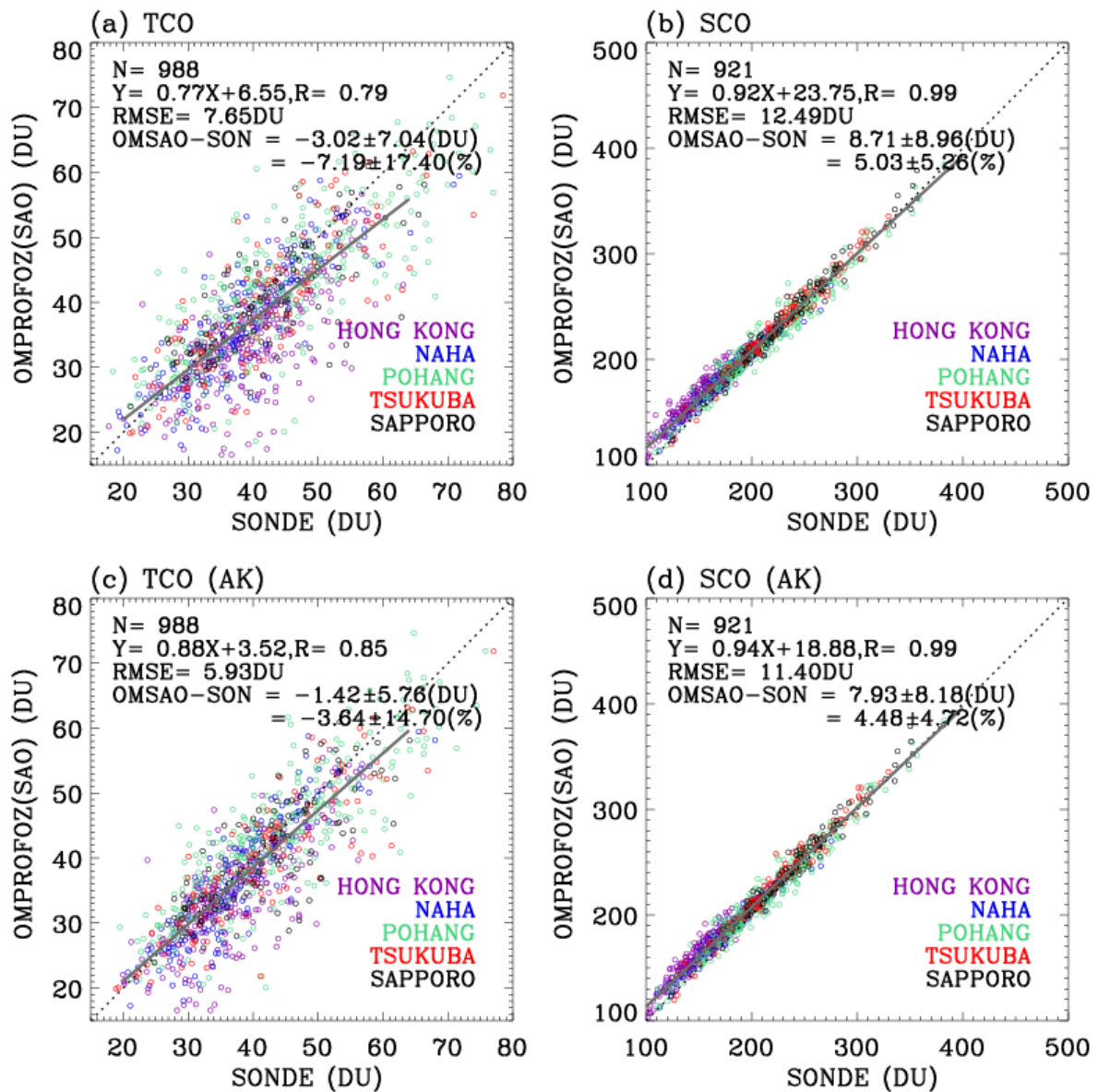
Figure 10. Same as Fig. 8, but for validating OMI research ozone profiles (OMPROFOZ) produced by the SAO OE-based algorithm.

Table1. List of ozonesonde stations**.**

Station[a]	Lon (°), Lat (°)	Altitude (m)	Observation Time [b]		Instrument Type[c]	ECC-SST [d]	Post Correction
Singapore	103.9, 1.3	40	07:30-08:00 (9)	Jan 12 - Sep 15	ECC/EN-SCI Z	SST0.5	No correction
				Nov15 - Dec15	ECC/SPC 6A		
Kuala Lumpur	101.7, 2.7	20	9:30-15:00 (104)	Jan 13 - Dec14	ECC/SPC 6A	SST1.0	Transfer function
				Jan 15 - Dec15	ECC/EN-SCI Z	SST0.5	
Trivandrum	77.0, 8.5	60	14:00-14:30 (34)	Jan 06 - Dec11	MBM		Correction factor
Hanoi	105.8, 21.0	10	12:00-14:00 (42)	Jan 05 - Apr 06	ECC/EN-SCI 1Z	SST2.0	Transfer function
				Apr06 - Dec 07	ECC/EN-SCI 2Z	SST2.0	
				Jan 08 - May 09	ECC/EN-SCI 2Z	SST1.0	
				Jun 09 - Dec 09	ECC/SPC 6A	SST1.0	
				Feb 10 - Dec 11	ECC/EN-SCI Z	SST1.0	
				Feb 12 - Dec 13	ECC/EN-SCI Z	SST2.0	
				Jan 15 - Dec 15	ECC/EN-SCI Z	SST0.5	
Hong Kong	114.1, 22.3	70	13:00-14:30 (11)	Jan 05 - Dec 15	ECC/SPC 6A	SST1.0	No correction
Naha	127.7, 26.2	30	14:30-15:00 (06)	Jan 05 - Oct 08	CI/ KC-96		Correction factor
				Nov 09 - Dec 15	ECC/EN-SCI 1Z	SST0.5	
New Delhi	77.1, 28.3	270	11:00-14:30 (69)	Feb 06 - Dec11	MBM		Correction factor
Pohang	129.2, 36.0	40	13:30-15:30 (24)	Jan 05 - Dec 15	ECC/SPC 6A	SST1.0	No correction
Tsukuba	140.1, 36.1	330	14:30-15:00 (08)	Jan 05 - Nov 09	CI/ KC-96		Correction factor
				Dec 09 - Dec 15	ECC/EN-SCI 1Z	SST0.5	
Sapporo	141.3, 43.1	30	14:30-15:00 (06)	Jan 05 - Nov 09	CI/ KC-96		Correction factor
				Dec 09 - Dec 15	ECC/EN-SCI 1Z	SST0.5	

[a] Data are downloaded from the WOUDC (http://woudc.org) data archive, except for Kuala Lumpur and Hanoi, which are from the SHADOZ (https://tropo.gsfc.nasa.gov/shadoz/) network, and Pohang, which are from the Korea Meteorological Administration (KMA).

[b] The range of the observation time (LT) with 1σ standard deviations of them (min) in parentheses.
[c] Ozonesonde sensor type (ECC: Electrochemical Condensation Cell, CI: Carbon iodine cell Japanese sonde, MBM: Modified Brewer-Mast Indian sonde). ECC sensors manufactured by either ECC sensor manufactures; Science Pump Corporation (Model type: SPC-6A) and Environmental Science cooperation (Model type EN-SCI-Z/1Z/2Z).
[d] Potassium Iodide (KI) cathode sensing solution type (SST) implemented in ECC ozone sensors: SST0.5 (0.5 % KI, half buffer), SST1.0 (1.0 % KI, full buffer), and SST 2.0 (2.0 % KI, no buffer). Singapore station changed it to SST1.0 as of 2018.

Table 2. Comparison statistics (mean bias in DU, 1σ standard deviation in DU, and *R*, correlation coefficient) between GEMS simulated tropospheric ozone column and ozonesonde measurements convolved with GEMS averaging kernels.

Station	Collocation Time difference	Type	Data Period (Year)	SONDE AK – GEMS		
				#	Mean Bias + 1σ	R
Singapore	6:44	ECC	12-15	20	-13.67 $\pm$ 9.61	0.17
Kuala Lumpur	2:29	ECC	05-15	106	-2.54 $\pm$ 4.13	0.44
Trivandrum	1:46	MBM	06-11	37	3.55 $\pm$ 9.75	0.24
Hanoi	0:32	ECC	05-15	100	-3.82 $\pm$ 6.03	0.52
Hong Kong	0:27	ECC	05-15	259	-1.19 $\pm$ 3.91	0.82
Naha	0:47	CI	05-08	135	-5.48 $\pm$ 4.07	0.85
		ECC	08-15	166	-0.94 $\pm$ 3.22	0.91
New Delhi	1:46	MBM	06-11	39	-4.57 $\pm$ 13.36	0.24
Pohang	0:54	ECC	05-15	281	-0.75 $\pm$ 3.13	0.95
Tsukuba	1:56	CI	05-09	151	-2.98 $\pm$ 3.76	0.91
		ECC	09-15	154	-0.65 $\pm$ 3.53	0.94
Sapporo	2:18	CI	05-09	107	-3.43 $\pm$ 2.56	0.94

ECC	09-15	95	-1.37 ± 2.79	0.93